Available online at www.eccomasproceedia.org
Eccomas Proceedia COMPDYN (2025) 769-779

ECCOMAS
Proceedia

COMPDYN 2025
10th ECCOMAS Thematic Conference on
Computational Methods in Structural Dynamics and Earthquake Engineering
M. Papadrakakis, M. Fragiadakis (eds.)
Rhodes Island, Greece, 15-18 June 2025

INCORPORATING SPATIAL CORRELATION IN PROBABILISTIC LOSS ASSESSMENT: AN IMPROVED CONVOLUTION-BASED METHOD WITH A CASE STUDY

Onur Ulku[1], **Ufuk Yazgan**[2], **and Sinan Akkar**[3]

[1]Department of Structures for Engineering and Architecture, University of Naples "Federico II", Italy
via Claudio 21, 80125 Napoli
e-mail: onur.ulku@unina.it

[2] Disaster Management Institute, Istanbul Technical University, Turkiye
Resitpasa, 34485, İstanbul
e-mail: ufukyazgan@itu.edu.tr

[3] T Rupt Technology Inc., Turkiye
Maslak Mah. Tasyoncası Sk, 34398, Istanbul
e-mail: sakkar@trupt.com.tr

Abstract. *Catastrophic risk management requires a comprehensive understanding of aggregate loss distribution, as well as an in-depth knowledge of the uncertainties influencing the reliability of this distribution. Aggregate loss distribution is particularly sensitive to uncertainties arising in hazard assessment processes and the vulnerability of building typologies. Traditionally, simulation-based methods are employed to estimate and analyze aggregate loss distribution, as these methods enable the modelling of complex uncertainties in hazard exposure and vulnerability. However, simulation-based approaches come with notable limitations: they are computationally intensive and time-consuming, particularly when analyzing large asset portfolios and attempting to calculate the tail of the loss distribution. Therefore, an alternative framework is proposed to calculate aggregate loss distribution using a convolution-based approach grounded in the total probability theorem. This framework is further enhanced by incorporating spatial correlation in intra-event shaking intensity, which is crucial for calculating aggregate loss in low exceedance probabilities for large portfolios. The improved convolution-based and simulation-based methods are applied to a portfolio in Zeytinburnu, Istanbul. The results demonstrate that the improved convolution-based method not only provides a more computationally efficient method but also offers more reliable aggregate loss in the tails of the distribution compared to the conventional simulation-based method. This framework offers a valuable tool for enhancing decision-making in risk transfer and mitigation efforts.*

Keywords: Probabilistic Loss Assessment, Convolution-based Loss Assessment, Simulation-based Loss Assessment, Earthquake Engineering, Spatial Correlation.

Peer-review under responsibility of the organizing committee of COMPDYN 2025.
doi: 10.7712/120125.12446.25284

1 INTRODUCTION

Earthquake-induced exposure losses are typically divided into three categories, which include casualties, direct losses and indirect losses. Direct losses refer to physical damage affecting structural and non-structural components and contents, along with the repair costs necessary to restore their functionality. These losses may also include the insured value of the building, which covers compensation for structural, non-structural and content damage. Indirect losses arise from the partial or complete disruption of the building's intended function due to physical damage to the structure itself or surrounding infrastructure, leading to business interruption and disruptions in social services that depend on the building functionality. Hereby, direct loss will be our focus for loss analysis. However, the method that we propose in the paper can also be utilized to aggregate indirect losses.

Effective management of catastrophic risk during the recovery process, as well as risk transfer and reduction strategies, requires a comprehensive understanding of aggregate loss distribution. These strategies often rely on the target exceedance probability of loss distribution. A key component of this process is recognizing the epistemic uncertainties and aleatoric variabilities within the seismic hazard, vulnerability and exposure models, as these factors influence the reliability of loss distribution.

In seismic hazard models, uncertainties are associated with parameters such as ground motion intensity measures (GMIM), rupture location along a source, source geometry and maximum magnitude of a source. Vulnerability models, on the other hand, introduce epistemic uncertainties due to a lack of detailed information on building characteristics, leading to variations in damage ratios. In this study, aleatoric variability in GMIM and epistemic uncertainty in damage ratio at a given GMIM are considered.

In the literature, numerous Ground Motion Models (GMMs) establish relationships between source-to-site distance, event magnitude, faulting mechanism, local soil conditions and other explanatory variables. GMIM is generally observed to follow a lognormal distribution, with its standard deviation comprising of two components: intra-event variability (σ_{intra}), which describes dispersion within a single event, and inter-event variability (σ_{inter}), which describes dispersion across different events. However, GMMs do not account for the intra-event spatial correlation between sites of interest. While this is not essential for single-site assessments, it becomes crucial when evaluating loss distributions for spatially distributed portfolios.

Two conventional methodologies are widely used to incorporate these uncertainties and variabilities in loss assessment, enabling the modelling of complex uncertainties in hazard, exposure and vulnerability. These include simulation-based loss assessment [1, 2] and convolution-based loss assessment [3, 4, 5]. Each approach has its advantages and limitations.

Simulation-based techniques, such as Monte Carlo simulations, are well suited for capturing uncertainties and implementing spatial ground-motion correlation within events. However, these methods struggle with accurately representing low probability exceedances, which influence the tail value losses. Addressing this limitation often requires significant computational resources, making these techniques time-consuming and costly.

Conversely, the convolution-based approach proposed by [3] accounts for the full distribution of GMIM and damage ratio at a given GMIM level. This method aggregates loss distributions by convolving two or more distributions using Fast Fourier Transformation (FFT). However, the convolution-based approach does not incorporate spatial ground motion correlation between the sites, which can significantly impact loss estimates for closely distributed exposures.

To address this gap, an improved convolution-based probabilistic loss assessment method is proposed by incorporating spatial correlation in ground motion fields. This study considers only intra-event spatial correlation and does not account for cross-correlation. Furthermore, the proposed method and its application will be demonstrated through a case study on a portfolio located in Zeytinburnu, Istanbul.

2 PROPOSED METHOD

Given an earthquake scenario, the proposed method is explained by considering a single asset at each site i, for i=1,. . . ,s. The earthquake scenario is described with a specific magnitude (M=m), source-to-site distance (R_i=r), and other explanatory variables (θ). Later, the inter-event variability is considered as a set of discrete ϵ_{inter} values covering the entire range of the standard normal distribution $\mathcal{N}\,(0,\,1)$ and aggregated with the Total Probability Theorem. We can write the loss probability density function (pdf) conditioned on these explanatory variables at site i when loss variability for each asset and intra-event variability is represented as:

$$f(l_i \mid M, D_i, \theta, \varepsilon_{\text{inter}}) = \int_0^\infty f_l(l_i \mid \text{IM} = im)\, f_{\text{IM}}(im \mid M, D_i, \theta, \varepsilon_{\text{inter}})\, \mathrm{d}im \tag{1}$$

where $f_l(l_i \mid \text{IM} = im)$ represents the conditional probability density function of a vulnerability function for a given intensity measure (IM) while $f_{\text{IM}}(im \mid M, D_i, \theta)$ denotes the probability density function of IM conditioned on explanatory variables, which can be defined as $\mathcal{N}\left(\ln(\overline{\text{IM}}),\, \sigma_{\text{intra}}\right)$.

2.1 One Site Multiple Assets

When site i contains a set of n assets, different correlation scenarios can be considered in terms of the damage ratio, particularly for risks that are classified within the same typology. If all assets are assumed to sustain the same level of damage, the damage ratios are fully correlated. Conversely, if each asset is affected independently, the damage ratios are uncorrelated. In practice, the correlation typically falls somewhere between these two extremes, influenced by factors such as spatial proximity between the assets and their structural similarity.

For simplicity, we assume that the damage ratio for each asset within the same typology is independent due to the lack of information on whether the assets belong to the same building within the portfolio. Additionally, in terms of intra-event variability, since all assets are located at the same site, no intra-event variability exists among them. Consequently, ϵ_{intra} should be assigned the same value for each asset, following a standard normal distribution ($\mathcal{N}\,(0,\,1)$). As a result, the ground motion u_i is given by Eq. (2).

$$u_i = \exp\left(\ln(\overline{\text{IM}}) + \varepsilon_{\text{inter}}\, \sigma_{\text{inter}} + \varepsilon_{\text{intra}}\, \sigma_{\text{intra}}\right) \tag{2}$$

Since losses for each asset are expected to be independent variables when conditioned on the ground motion, convolution can be applied to aggregate the loss distributions of individual assets. Consequently, the total loss probability density function for a set of assets within the same site can be determined using the convolution of the conditional probability density functions of asset losses, as expressed in Eq. (3).

$$f_{l_T}(l_i \mid u_i) = \left(f_{1|u_i} * f_{2|u_i} * \cdots * f_{n|u_i}\right) \tag{3}$$

The term $f_{1,2,\ldots,n|u_i}$ represents the loss distribution of each asset conditioned on the ground motion intensity u_i. The symbol $*$ denotes the convolution operation. The exceedance probability, represented by the complementary cumulative distribution function (CCDF) for a given loss threshold conditioned on intra-event variability, can be determined by integrating Eq. (3) over the total loss distribution, taking into account all assets located within the site.

$$P(L_T > l \mid \varepsilon_{\text{inter}}, \varepsilon_{\text{intra}}) = 1 - \int_0^l f_{l_T}(l_i \mid u_i)\,\mathrm{d}l \tag{4}$$

Eq. (5) represents the exceedance probability of a specific aggregated loss threshold when a single site contains multiple assets. This formulation accounts for the total loss distribution by considering the contributions of all assets at the site of interest.

$$P_L^T(L_T > l \mid \varepsilon_{\text{inter}}) = \int_{-\infty}^{\infty} P(L_T > l \mid \varepsilon_{\text{inter}}, \varepsilon_{\text{intra}})\, f_{\varepsilon_{\text{intra}}}(\varepsilon_{\text{intra}})\,\mathrm{d}\varepsilon_{\text{intra}} \tag{5}$$

2.2 Multiple Sites

Exposures are generally distributed over a geographic area, making it usual (compulsory) to consider multiple sites in loss assessment. As previously mentioned, when multiple sites are involved, the spatial correlation of intra-event variability begins to influence the aggregated loss distribution, particularly when the sites are close to each other. Therefore, the spatial correlation of intra-event variability should be accounted for based on the distance between sites (inter-site distance). This correlation can be represented by using a multivariate normal distribution, given that $\varepsilon_{\text{intra}}$ follows a standard normal distribution. Consequently, the multivariate normal distribution $\mathcal{N}(\mu, \Sigma)$ of intra-event variability can be modelled as follows:

$$\mu = [0 \;\; 0 \;\; \cdots \;\; 0]_{1\times s} \tag{6}$$

$$\Sigma = \begin{bmatrix} 1 & \rho_{1,2}(h) & \cdots & \rho_{1,s}(h) \\ \rho_{2,1}(h) & 1 & \cdots & \vdots \\ \vdots & \vdots & \ddots & \vdots \\ \rho_{s,1}(h) & \rho_{s,2}(h) & \cdots & 1 \end{bmatrix}_{s\times s} \tag{7}$$

where μ is a conditional mean vector, and Σ is the covariance matrix of the multivariate normal distribution. Moreover, $\rho(h)$ represents the spatial correlation as a function of the inter-site distance h between the sites. This correlation describes how intra-event variability is related across different locations, with higher correlation values typically observed for sites that are closer together and lower values for those farther apart. Several studies have been conducted to determine spatial correlation, including those by [6], [7], and [8]. In this paper, we adopt the [6] model [Eq. (8)] along with its associated parameters, which are a, b, and c, to account for spatial correlation in intra-event variability. So, Eq. (5) transforms into Eq. (9) by incorporating Eq. (3).

$$\rho(h) = \max\left\{(1-c) + e^{-ah^b},\, 0\right\} \tag{8}$$

$$P_{L_T}(L_T > l \mid \varepsilon_{\text{inter}}) = \int_{\varepsilon_{\text{intra}_s}=-\infty}^{\infty} \cdots \int_{\varepsilon_{\text{intra}_1}=-\infty}^{\infty} P\left(L_T > l \mid \varepsilon_{\text{inter}}, \varepsilon_{\text{intra}_1}, \ldots, \varepsilon_{\text{intra}_s}\right) \times f\left(\varepsilon_{\text{intra}_1}, \ldots, \varepsilon_{\text{intra}_s}\right) \, d\varepsilon_{\text{intra}_1} \cdots d\varepsilon_{\text{intra}_s} \tag{9}$$

where $f(\varepsilon_{\text{intra}_1}, \ldots, \varepsilon_{\text{intra}_s})$ is a multivariate probability density function with the mean μ and the covariance Σ.

2.3 Multiple Sites and $\varepsilon_{\text{inter}}$

The proposed method can also account for a set of $\varepsilon_{\text{inter}}$ by incorporating the full distribution of inter-event variability, which also follows a standard normal distribution. In Eq. (9), the formula is derived for a specific $\varepsilon_{\text{inter}}$. However, when inter-event variability is considered, Eq. (9) transforms into Eq. (10) to reflect this uncertainty.

$$P_{L_T}(L_T > l) = \int_{\varepsilon_{\text{inter}}=-\infty}^{\infty} \int_{\varepsilon_{\text{intra}_s}=-\infty}^{\infty} \cdots \int_{\varepsilon_{\text{intra}_1}=-\infty}^{\infty} P\left(L_T > l \mid \varepsilon_{\text{inter}}, \varepsilon_{\text{intra}_1}, \ldots, \varepsilon_{\text{intra}_s}\right) \times f\left(\varepsilon_{\text{intra}_1}, \ldots, \varepsilon_{\text{intra}_s}\right) f(\varepsilon_{\text{inter}}) \, d\varepsilon_{\text{inter}} \, d\varepsilon_{\text{intra}_1} \cdots d\varepsilon_{\text{intra}_s} \tag{10}$$

where $f(\varepsilon_{\text{inter}})$ is the probability density function of the standard normal distribution. It should be noted that intra-event and inter-event variability are assumed to be independent of each other.

However, the method cannot be implemented by treating $\varepsilon_{\text{inter}}$ and $\varepsilon_{\text{intra}}$ as continuous variables due to current computational limitations. Therefore, discrete random variables are used to approximate the full distributions by considering values within the range of -2 to $+2$ standard deviations, with increments of 0.5. This discretization is feasible for representing the variation in $\varepsilon_{\text{inter}}$ and $\varepsilon_{\text{intra}}$, ensuring a balance between accuracy and efficiency in the numerical implementation. As a result, Eq. (10) can be expressed as:

$$P_{L_T}(L_T > l) = \sum_{\varepsilon_{\text{inter}}=-2}^{2} \sum_{\varepsilon_{\text{intra}_s}=-2}^{2} \cdots \sum_{\varepsilon_{\text{intra}_1}=-2}^{2} P\left(L_T > l \mid \varepsilon_{\text{inter}}, \varepsilon_{\text{intra}_1}, \ldots, \varepsilon_{\text{intra}_s}\right) \times p\left(\varepsilon_{\text{intra}_1}, \ldots, \varepsilon_{\text{intra}_s}\right) p(\varepsilon_{\text{inter}}) \tag{11}$$

where $p(\varepsilon_{\text{intra}_1}, \ldots, \varepsilon_{\text{intra}_s})$ represents the probability mass function (pmf) of a multivariate normal distribution, while $p(\varepsilon_{\text{inter}})$ denotes the pmf of a truncated standard normal distribution bounded between -2.5 and 2.5.

In the next chapter, this method will be applied to a portfolio consisting of three sites located in the Zeytinburnu district of Istanbul to demonstrate the potential impact of ground motion spatial correlation on loss distribution. Additionally, each site in the district contains a set of accumulated assets. This application enables the evaluation of the full correlation of ground motion within each site, spatial correlation effects across different sites, and the aggregation of loss distributions across multiple locations.

3 APPLICATION

The Zeytinburnu district in Istanbul was selected for this study due to the anticipated risk of a devastating earthquake along the North Anatolian Fault. Numerous studies have highlighted the likelihood of an earthquake exceeding magnitude 7 in the Marmara Sea following the 1999 earthquakes in the Düzce and Kocaeli provinces [9, 10, 11, 12, 13, 14, 15, 16]. The seismic scenario considered for the loss assessment involves an earthquake with a moment magnitude of 7.07 occurring in the Central Marmara segment of the North Anatolian Fault. The selected event, as proposed by [9], represents the 50th percentile of the probability of occurrence.

For analytical purposes, the Zeytinburnu district was divided into three subareas, each approximately two kilometres apart (see Figure 1). A total of 12,808 assets, which refers to policies insured by TCIP, within Zeytinburnu were assigned to the centre of the nearest subarea based on their geographical proximity. Additionally, as a preliminary analysis to demonstrate the feasibility of the approach, all buildings within Zeytinburnu were assumed to be low-rise reinforced concrete (RC) structures constructed between 1980 and 2000 (mid-code classification), aligning with the selected vulnerability model. The vulnerability model corresponding to this typology was retrieved from the GEM Vulnerability Library [17]. However, insured values varied across assets due to differences in floor area.

The intensity measure, spectral acceleration at 0.3 seconds $S_a(T = 0.3s)$, was computed for the specified seismic event at both the actual coordinates of the buildings and the centres of the subareas using the ground motion model (GMM) developed by Akkar et al. [18] via the OpenQuake Platform [19]. Figure 1 also presents a heatmap illustrating the spatial distribution of the median $S_a(T = 0.3s)$ values at the actual building coordinates. However, as previously mentioned, for the calculations, the intensity value at the centre of each subarea, along with its intra-event and inter-event variability, was considered for all assets within that subarea.

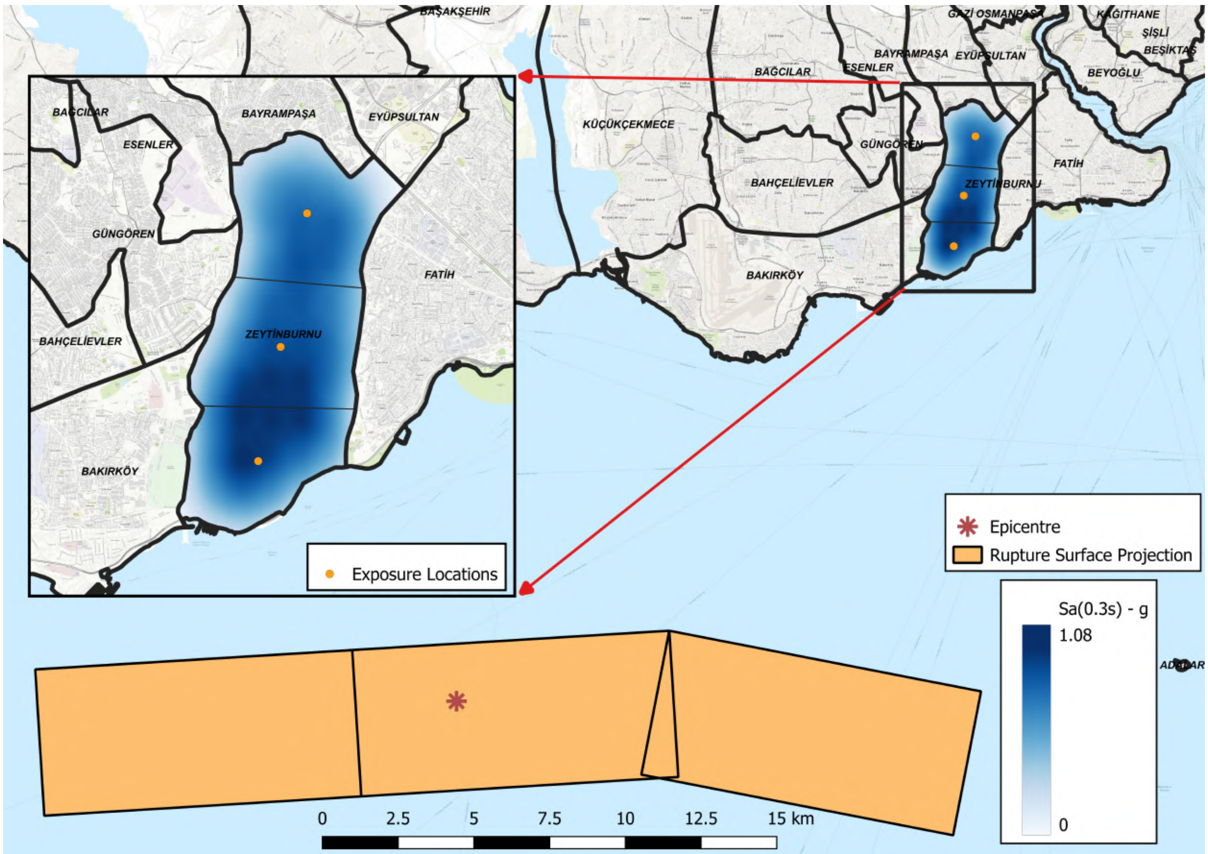

Figure 1: Location of assets and map of ground shaking.

Additionally, it should be noted that all assets located at the same site are assumed to be fully correlated in terms of ground motion but independent in terms of loss ratio. Consequently, the total loss distribution for all assets at the same site was computed using Eq. (4), while Eq. (11) was applied to aggregate the loss distribution across different locations, accounting for the spatial correlation between sites. The parameters and models for spatial correlation were adopted from Jayaram and Baker [6].

The algorithms were coded in Python, and calculations were performed on a system equipped with a 13th-generation Intel Core i9 processor, 32 GB of RAM, and an NVIDIA GeForce RTX 4060 GPU.

4 RESULTS

The loss distributions computed using the proposed method were compared with those obtained through a Monte Carlo simulation-based approach to highlight the differences and similarities between convolution-based and simulation-based methods. In the Monte Carlo simulation, 1,000 inter-event epsilon values were generated. For each simulation run, one intra-event epsilon was sampled for each site, either randomly (uncorrelated intra-event) or with spatial correlation, depending on the comparison case. Additionally, one damage ratio was randomly sampled for each asset, reflecting the assumption of independence among assets in terms of damage ratio. The mean of the 1,000 loss distributions, each obtained from an inter-event simulation, was then calculated and included in the comparisons to illustrate the variability inherent in Monte Carlo simulations, a well-documented limitation of simulation-based methods, particularly in capturing the tail of the distribution. To assess the impact of the proposed model and the role of spatial correlation, three comparative analyses were conducted:

- (a) a comparison of uncorrelated and spatially correlated convolution-based loss distributions (Figure 2),
- (b) a comparison of uncorrelated Monte Carlo and convolution-based loss distributions (Figure 3), and
- (c) a comparison of spatially correlated Monte Carlo and convolution-based loss distributions (Figure 4).

Comparison (a) demonstrates the effect of incorporating spatial correlation into convolution-based calculations, while (b) evaluates the differences in convolution-based loss distribution and a simulation-based approach. Finally, (c) examines the differences between the proposed convolution-based loss distribution, which accounts for spatial correlation, and the simulation-based loss distribution.

Figure 2 illustrates that higher losses are observed at low exceedance probabilities when considering spatial correlation. At high exceedance probabilities, the difference between the correlated and uncorrelated cases becomes negligible, and in some cases, losses may even be slightly lower with spatial correlation. Although the effect of spatial correlation is not apparent in average losses, it becomes increasingly significant for loss thresholds associated with low exceedance probabilities. This result is highly consistent with findings in the literature [20].

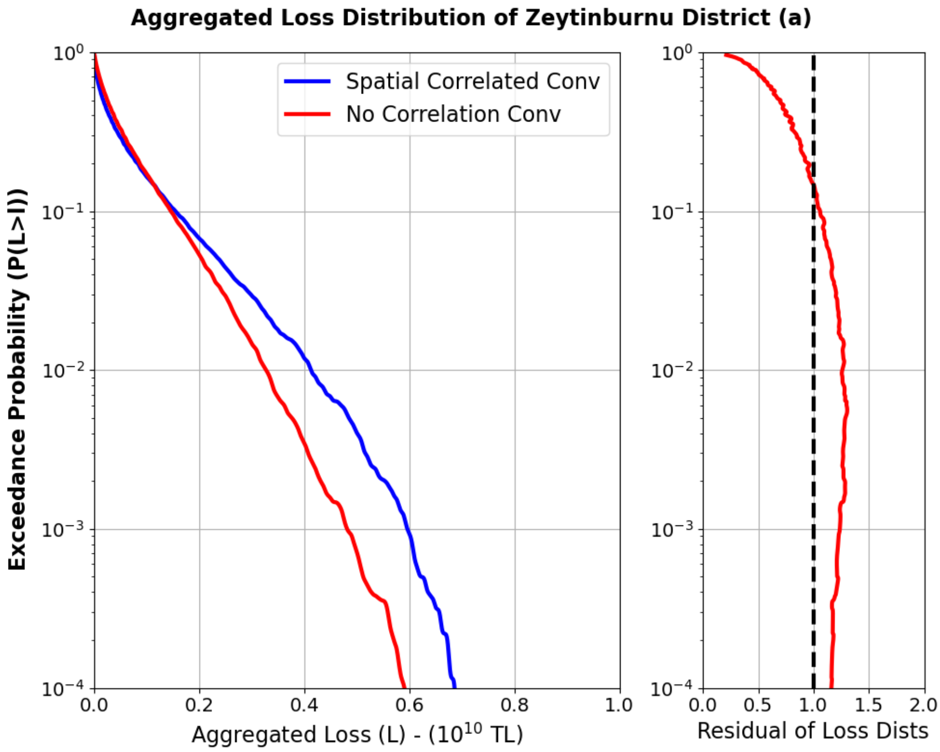

Figure 2: Comparison of aggregated loss distributions considering spatial correlation versus no correlation.

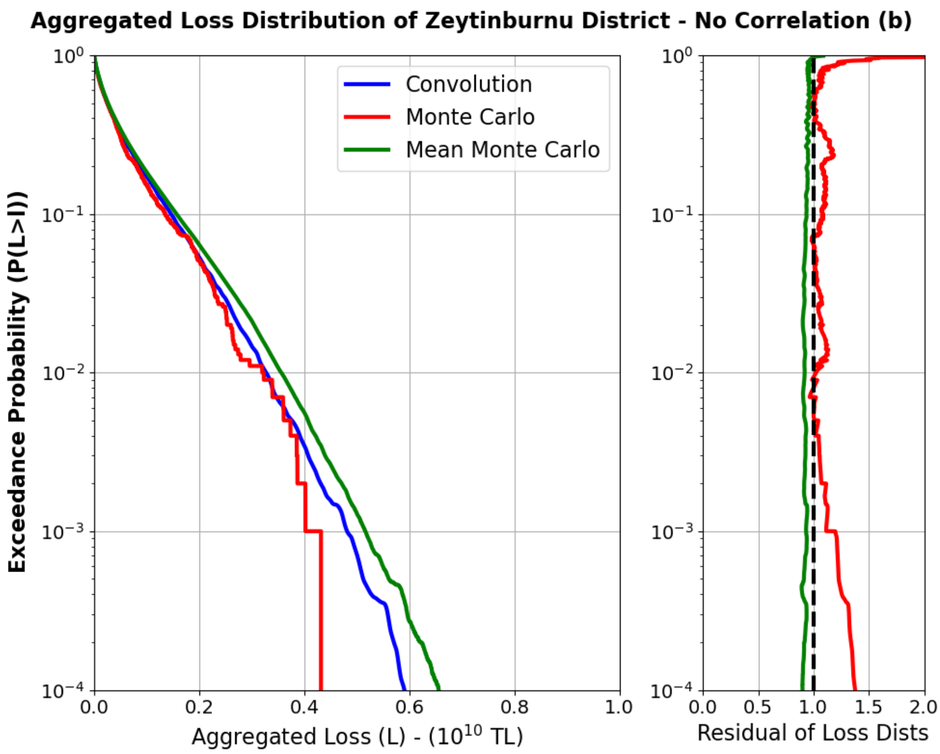

Figure 3: Comparison of aggregated loss distributions obtained with MCS and Convolution without considering spatial correlation.

Figure 3 demonstrates that the Monte Carlo Simulation (MCS) method can yield varying loss distributions across different runs, potentially leading to uncertainty and reduced reliability. To address this issue, the simulation should be repeated multiple times, and the mean of the resulting distributions should be taken to achieve more stable and reliable outcomes. However, this repetition increases computational cost and slows down the process. As shown in Figure 3, the mean of the Monte Carlo simulations closely aligns with the results obtained from the convolution-based approach. The minor differences observed may be attributed to the use of discrete rather than continuous representations for intra-event and inter-event variability.

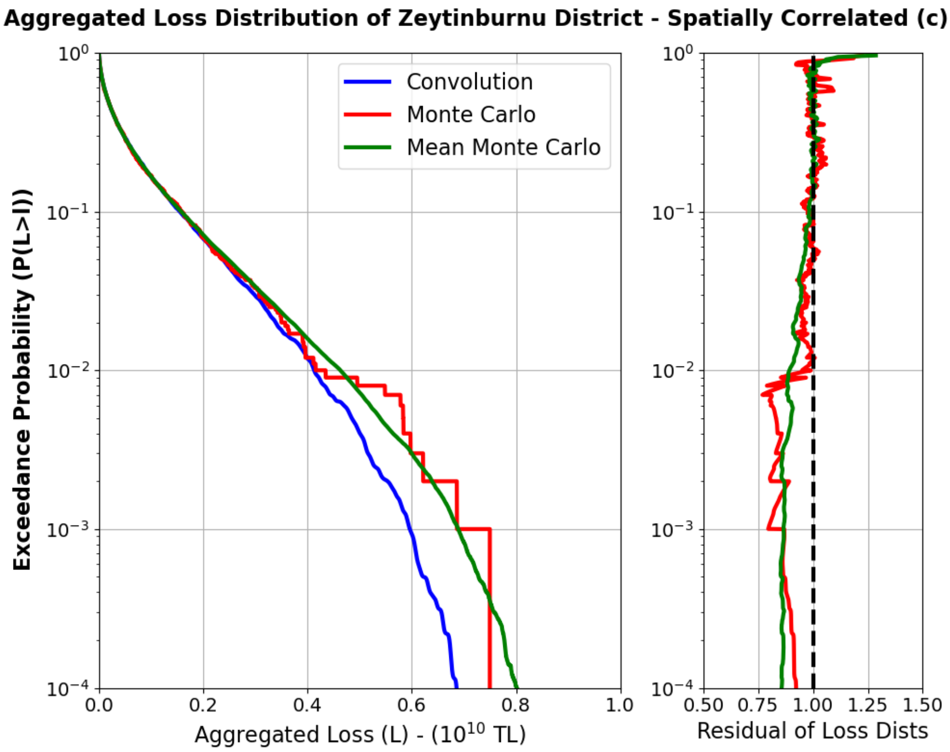

Figure 4: Comparison of aggregated loss distributions obtained with MCS and Convolution considering spatial correlation.

Figure 4 clearly highlights that, although spatial correlation adds complexity to the modelling process, the convolution method remains a robust and computationally efficient alternative to repeated simulations, which may otherwise exhibit significant run-to-run variability.

5 CONCLUSION

The results show how important it is to consider spatial correlation for aggregated loss distributions, especially at the tail of the distribution (low exceedance probabilities). This effect can have significant implications for many sectors, particularly the re/insurance industry. While Monte Carlo Simulation is commonly used, it introduces variability across runs and requires repeated sampling to achieve stable results, which increases the computational burden. In contrast, the proposed convolution-based approach proves to be more reliable and efficient, as it captures the full distribution of asset damage without the need for multiple simulations. For further improvement, incorporating spatial cross-correlation into the proposed method could enhance its accuracy, especially when modelling geographically diverse and heterogeneous portfolios.

REFERENCES

[1] R.M.W. Musson, The use of Monte Carlo simulations for seismic hazard assessment in the U.K., *Annals of Geophysics*, **43(1)**, 2000.

[2] V. Silva, H. Crowley, M. Pagani, D. Monelli, R. Pinho, Development of the OpenQuake engine, the Global Earthquake Model's open-source software for seismic risk assessment, *Natural Hazards*, **72(3)**, 1409–1427, 2013.

[3] R.L. Wesson, D.M. Perkins, N. Luco, E. Karaca, Direct calculation of the probability distribution for earthquake losses to a portfolio, *Earthquake Spectra*, **11(1)**, 687–706, 2009.

[4] U. Yazgan, S. Akkar, O. Ulku, Estimating Aggregate Earthquake Losses to Insurance Portfolios Using Convolution Approach, *12th US National Conference on Earthquake Engineering*, Salt Lake City, Utah, 27 June – 1 July, 2022.

[5] S. Akkar, U. Yazgan, O. Ulku, Earthquake loss models in Turk Reinsurance Inc.'s catastrophic event modeling platform for portfolio losses, *3rd European Conference on Earthquake Engineering and Seismology*, Bucharest, Romania, 2022.

[6] N. Jayaram, J.W. Baker, Correlation model for spatially distributed ground-motion intensities, *Earthquake Engineering & Structural Dynamics*, **38(15)**, 1687–1708, 2009.

[7] K. Goda, H.P. Hong, Spatial correlation of peak ground motions and response spectra, *Bulletin of the Seismological Society of America*, **98(1)**, 354–365, 2008.

[8] M. Wang, T. Takada, Macrospatial correlation model of seismic ground motions, *Earthquake Spectra*, **21(4)**, 1137–1156, 2005.

[9] M. Murru, A. Akinci, G. Falcone, S. Pucci, R. Console, T. Parsons, M 7 earthquake rupture forecast and time-dependent probability for the Sea of Marmara region, Turkiye, *Journal of Geophysical Research: Solid Earth*, **121**, 2679–2707, 2016.

[10] A. Hubert-Ferrari, A. Barka, E. Jacques, S. Nalbant, B. Meyer, R. Armijo, P. Tapponnier, G.C.P. King, Seismic hazard in the Marmara Sea following the 17 August 1999 Izmit earthquake, *Nature*, **404**, 269–272, 2000.

[11] T. Parsons, S. Toda, R.S. Stein, A. Barka, J.H. Dieterich, Heightened odds of large earthquakes near Istanbul: An interaction-based probability calculation, *Science*, **288**(5466), 661–665, 2000.

[12] T. Parsons, Recalculated probability of Mw = 7 earthquakes beneath the Sea of Marmara, Turkey, *Journal of Geophysical Research*, **109**(5), 2004.

[13] K. Atakan, A. Ojeda, M. Meghraoui, A. Barka, M. Erdik, A. Bodare, Seismic hazard in Istanbul following the August 17, 1999 Izmit and November 12, 1999 Düzce earthquakes, *Bulletin of the Seismological Society of America*, **92**(1), 466–482, 2002.

[14] M. Erdik, M. Demircioglu, K. Sesetyan, E. Durukal, B. Siyahi, Earthquake hazard in Marmara Region, Turkey, *Soil Dynamics and Earthquake Engineering*, **24**(8), 605–631, 2004.

[15] E. Kalkan, P. Gulkan, N. Yilmaz, M. Celebi, Reassessment of probabilistic seismic hazard in the Marmara Region, *Bulletin of the Seismological Society of America*, **99**(4), 2127–2146, 2009.

[16] Z. Gülerce, S. Ocak, Probabilistic seismic hazard assessment of Eastern Marmara Region, *Bulletin of Earthquake Engineering*, **11**(5), 1259–1277, 2013.

[17] L. Martins, V. Silva, Global Vulnerability Model of the GEM Foundation, *GitHub*, 2023

[18] S. Akkar, M.A. Sandikkaya, J.J. Bommer, Empirical Ground-Motion Models for Point- and Extended-Source Crustal Earthquake Scenarios in Europe and the Middle East, *Bulletin of Earthquake Engineering*, **12**(1), 359–387, 2014.

[19] M. Pagani, D. Monelli, G. Weatherill, L. Danciu, H. Crowley, V. Silva, P. Henshaw, L. Butler, M. Nastasi, L. Panzeri, M. Simionato, D. Vigano, OpenQuake Engine: An Open Hazard (and Risk) Software for the Global Earthquake Model, *Seismological Research Letters*, **85**(3), 692–702, 2014.

[20] G.A. Weatherill, V. Silva, H. Crowley, P. Bazzurro, Exploring the impact of spatial correlations and uncertainties for portfolio analysis in probabilistic seismic loss estimation, *Bulletin of Earthquake Engineering*, **13**(4), 957–981, 2015.